Finite Diffusion Multi-Components Fuel Droplet Vaporization Modeling Using Continuous Thermodynamics for Fuels with Distinct Composition Distributions

C. Shen[1], W.L. Cheng[1], C. F. Lee[1,2*]
[1]Department of Mechanical Science and Engineering, University of Illinois at Urbana-Champaign, USA
[2]Center for Combustion Energy and State Key Laboratory of Automotive Safety and Energy, Tsinghua University, China;
caishen1@illinois.edu, waycheng@illinois.edu, and cflee@illinois.edu

Abstract

Commercial fuels are composed of hundreds of chemically different hydrocarbons. An accurate and efficient way to model the vaporization process is required to represent the droplet evaporation under typical engine operation condition. In this study, a finite diffusion droplet evaporation model for complex liquid mixture composed of different homogeneous groups is presented in this paper. Separate distribution functions are used to describe the composition of each homogeneous group in the mixture. Only a few parameters are required to describe the mixture. Quasi-steady assumption is applied in the determination of evaporation rates and heat flux to the droplet, and the effects of surface regression, finite diffusion and preferential vaporization of the mixture are included in the liquid phase equations using an effective properties approach. A novel approach was used to reduce the transport equations for the liquid phase to a set of ordinary differential equations. The proposed model was compared against experimental measurements for single, isolated droplets of n-decane, kerosene, heptane-decane and diesel-butanol. The proposed model predicted the temperature and droplet size variations well. The present model was applied to simulate the evaporation of isolated droplets with composition of typical diesel. Computations showed that the model captured the main distillation characteristics of commercial fuels reasonably well. The proposed model is capable in capturing the vaporization characteristics of complex liquid mixtures.

Introduction

Commercial fuels are mixtures of hundreds of chemically different hydrocarbons with vastly different boiling points that could range from 340 K to over 700 K. Law [1] pointed out that liquid motion within the droplet, miscibility among the liquid components and relative volatilities of the components are the three controlling factors in the understanding of the multi-component fuel behaviors. The immensely different volatilities among the components imply significant differences in the evaporation rates. Moreover, the liquid constituents can evaporate only if it reaches the surface. As the more volatile species evaporates, less volatile constituents become dominating within the liquid phase. As a result, the species mass fractions and temperature are no longer uniform within the droplet. This process is known as preferential evaporation. In most numerical simulations, the fuel is usually represented by a single component, for example, tetradecane ($C_{14}H_{30}$) is usually used to represent commercially available diesel. A major deficiency with this approach is that the influence of fuel composition is not accounted for, and, only the average evaporation behavior can be obtained. A possible solution to this is to use a set of fuel constituents to reproduce the distillation curve. An accurate representation of the fuel is essential for acquiring insightful information out of a simulation. The volatility of the fuel maintains a dominant position on spray penetration, and ignition is controlled by the most volatile species in the mixture [2, 3]. However, to represent each component in a commercial fuel, which consists of hundreds of component, using a discrete representation is impractical. Not only every component requires a separate transport equation, the exact composition is generally unknown.

As an alternative, continuous thermodynamics provides a more effective solution. The mixture is characterized by a probability distribution function (PDF) with respect to some characterizing variables, for examples, molecular weight or boiling points. Only a few parameters are required to describe the mixture, namely, the mean and variance of the probability distribution function. This approach was first developed in chemical engineering and has been applied in a variety of calculations including vapor-liquid equilibrium, liquid-liquid equilibrium, flash boiling and characterization of hydrocarbon mass fraction. It was first used for investigating the vaporization of isolated droplets by Tamim and Hallett [4]. The gas phase transport equations were solved with fine grid spacing close to the droplet surface. But this is infeasible for multi-dimensional spray simulations, which involve thousands of droplet parcels and complex engine geometry. Hallett [5] presented a quasi-steady

* Corresponding author: cflee@illinois.edu

analytical solution for droplet vaporization and applied his model to computations of diesel and gasoline, which captured important features, such as the distillation curves of commercial fuels, quite well. This model was extended to fuel droplet vaporization in a high-pressure environment [6]. The method of continuous thermodynamics has been applied in multi-dimensional engine modeling for spray calculations [7-11]. These studies made important contributions to the application of continuous thermodynamics to internal combustion engine simulations. However, most of the previous studies [9-18] are based on the assumption of infinite diffusion in the liquid phase, so non-uniformity inside the droplet is not considered.

The evaporation of fuel in high pressure ambient has been investigated extensively in the literature [12-16], since fuel evaporates in high-pressure ambient in many engineering applications. Ghassemi et al. [13, 14] reported the evaporation of droplets behaved differently at elevated ambient pressure. The evaporation of a bi-component droplet occurs in three stages, which was unseen from a single-component droplet. Most of the component with lower boiling point evaporated first, then, a non-evaporative heat-up process, followed by the evaporation of the less volatile component. There were attempts in modeling high-pressure evaporation of fuel droplets using zero-dimensional models, for applications in multi-dimensional engine simulations. Zhu and Aggarwal [17] studied the effects of equations of state on droplet transient evaporation and concluded that the Peng-Robinson equation of state predicted the droplet evaporation accurately. Aggarwal and Mongia [18] developed a high-pressure evaporation model accounting for multi-component effect. The study concluded that elevating ambient pressure lengthened the heat up process, but variation in ambient pressure did not visibly affect the droplet lifetime. Tonini et al. [19] presented a spray calculation using the high-pressure vaporization model by Aggarwal and Mongia [18]. The authors concluded that zero-dimensional models would provide enough accuracy in engine simulations, considering the uncertainties from droplet breakup and collision, vapor-phase turbulence and droplet-turbulence interactions in such calculations. Wang and Lee [20] proposed a model using the continuous thermodynamics formulation in order to account for high-pressure effects. Gas solubility imposed significant effects on the droplet breakup as it altered surface tension. Consequently, the predicted spray structure, fuel-vapor distribution and engine performance were considerably different than droplet evaporating at atmospheric ambient.

Numerical and/or Experimental Methods

In this paper, a comprehensive model considering preferential vaporization of a complex fuel mixture using continuous thermodynamics without the infinite diffusion assumption in the liquid phase is presented. This approach uses only three equations to trace the mass transfer process: one for the mole fraction, one for the first moment and another one for the second moment of the probability distribution function used to represent the mixture. Therefore, it eliminated the need to trace the evolution of each component independently. The improvement in computational efficiency is embedded in the mathematical formulation. This could be a significant improvement in computational efficiency especially in cases of complicated mixtures. The model consists of a gas phase sub-model which determines evaporation rates and heat flux, and a liquid phase sub-model with finite diffusion.

Gas Phase Model

A fuel mixture is described by a continuous probability distribution function, $f(\omega)$, characterized by the molecular weight, ω, of each component. The fraction of a component is $y_F f(\omega_i)\delta\omega$, where y_F is the total molar fraction of fuel in gas phase, and in this study, $f(\omega)$ is a Γ-distribution function, which is often used to represent petroleum fractions [20],

$$f(\omega) = \frac{(\omega-\gamma)^{\alpha-1}}{\beta^{\alpha}\Gamma(\alpha)} \exp\left(-\frac{\omega-\gamma}{\beta}\right), \quad (1)$$

where γ is the origin, α and β are parameters controlling the shape of the probability distribution function, with the mean molecular weight, $\theta_1 = \alpha\beta + \gamma$, and the variance, $\sigma^2 = \alpha\beta^2$. In previous studies, using the second moment, $\theta_2 = \sigma^2 + \theta_1^2$, was found to be more convenient for calculations than using the variance [4]. Here, θ_j is the j^{th} moment of $f(\omega)$. The transport equations for energy and molar fuel fraction, y_F, can be obtained by integrating energy and species conservation equations over the probability distribution function and two additional transport equations for θ_1 and θ_2 are achieved by performing proper weightings over the equation for fuel fraction. The gas phase transport equations for droplet vaporization, using continuous fuel representation, were first completed by Tamim and Hallett [4].

The methodology is similar to previously studies within the frame work of continuous thermodynamics. The vapor-phase quasi-steady solutions are given by:

$$\dot{N}'' = \frac{Sh_j}{2} \frac{C_{vap} D_{0_j}}{R} \ln(1 + B_j) , \quad (2)$$

$$\dot{N}''_{\Psi_j} = \dot{N}'' \left[\Phi_{j,R} - \frac{\Phi_{j,R} - \Phi_{j,\infty}}{1 - (1 + B_j)^{D_{0j}/D\Psi_j}} \right] , \quad (3)$$

where $\dot{N}''$ is the total vapor flux, and $\dot{N}''_{\psi_j}$ is the flux for j^{th} moment; D_{y_f} and D_{θ_j} is the average diffusivity for fuel composition and j^{th} moment, respectively, and B_j is the transfer number given by,

$$B_j = \frac{y_{j,surf} - y_{j,\infty}}{\frac{\dot{N}''_{\psi_j}}{\dot{N}''} - y_{j,\,surf}}. \tag{4}$$

Note that the Sherwood number is evaluated using fuel fraction, since the diffusivities for composition and the moments are almost the same. The heat flux to the droplet, $\dot{q}''$, is given by,

$$\dot{q}'' = \dot{N}'' \left[\frac{C_p (T_\infty - T_R)}{\exp\left(\frac{2\,\dot{N}''\,C_p R}{k_{vap} \cdot Nu} - 1 \right)} - \Delta H_{fg} \right], \tag{5}$$

where C_p, ΔH_{fg}, k_{vap} and Nu are the vapor phase specific heat capacity, latent heat for vaporization, thermal conductivity and Nusselt number, respectively.

Liquid Phase Model

The transient behavior of the liquid phase significantly affects the evaporation of a spray and thus, the vapor distribution. In the present study, an effort is made to properly model the non-uniformity of liquid phase due to finite diffusion vaporization rather than using the infinite diffusion model as in the study by Tamim and Hallett [4]. The transport equations for the liquid phase are obtained with the same approach as used in the gas phase. The complete liquid phase equations are too complex to be solved analytically. Previous studies on the liquid phase during droplet vaporization have provided a lot of knowledge and inspiration on the simplifications to the problem while retaining reasonable accuracy. Internal circulation enhances diffusion in the liquid phase and this effect can be accounted for by an effective diffusivity and conductivity [21, 22]. In addition, assuming that in a short time interval, molar concentration and specific heat are constant, and that the flow is symmetric since the effects of internal vortices are included in the effective properties [23], the liquid phase equations can then be simplified and written as:

$$\frac{\partial\, C_{liq} \vec{\Phi}}{\partial t} = \frac{1}{r^2} \frac{\partial}{\partial r} \left(r^2\, C_{liq}\, D_\Phi \frac{\partial \vec{\Phi}}{\partial r} \right), \tag{6}$$

where the subscript *liq* represents liquid phase, $\vec{\Phi}$ is a vector of $\{\Phi_j\}_{j=1}^{N}$. Note that the diffusivities in equation (6) are multi-component diffusivities, which are in general given by,

$$D_\Phi = B^{-1}, \tag{7}$$

for an ideal mixture. The elements of B are calculated from the binary diffusion coefficients and molar composition of the mixture as,

$$B_{ii} = \frac{y_i}{\mathcal{D}_{iN}} + \sum_{\substack{k=1 \\ i \neq k}}^{N} \frac{y_i}{\mathcal{D}_{ik}}, \; B_{ij} = -\, y_i \left(\frac{1}{\mathcal{D}_{ij}} - \frac{1}{\mathcal{D}_{iN}} \right). \tag{8}$$

The boundary conditions for liquid phase are given by,

$$\left.\frac{\partial \vec{\Phi}}{\partial r}\right|_{r=0} = 0, \; C_{liq} D_\Phi \left.\frac{\partial \vec{\Phi}}{\partial r}\right|_{r=R} = \dot{N}'' \vec{\Phi} - \vec{\dot{N}}''_{\Phi_j} = \vec{\Omega}_\Phi. \tag{9}$$

The conductivity and diffusivities in the equations are all effective properties. Symmetry imposes the boundary conditions at the droplet center, and conservation conditions are applied at the droplet surface,

$$\left.\frac{\partial \Phi}{\partial r}\right|_{r=0} = 0, \; C_{liq} D_\Phi \left.\frac{\partial \Phi}{\partial r}\right|_{r=R} = N_{Y_f}\, \Phi - N_\Phi = \Omega_\Phi. \tag{10}$$

Equation (6) represents a system of coupled partial differential equations, for which an exact, analytical solution is in general unavailable as the diffusivity matrix, D_Φ, strongly depends on mixture composition. The solution can be computationally intensive, even if efficient numerical techniques are employed. If C_{liq} and D_Φ are assumed constant, as in Toor [24] and Stewart and Prober [25],

$$C_{liq} \frac{\partial \vec{\Phi}}{\partial t} = C_{liq}\, D_\Phi \frac{1}{r^2} \frac{\partial}{\partial r} \left(r^2 \frac{\partial \vec{\Phi}}{\partial r} \right). \tag{11}$$

The system of equations can then be linearized and decoupled by decomposing the diffusivity matrix using eigenvalue decomposition. It has been shown that eigenvalue decomposition always exists for the diffusivity matrix [26],

$$\Lambda = \Sigma^{-1} D_\Phi\, \Sigma, \tag{12}$$

where Λ is the diagonal eigenvalue matrix, and Σ is the associated eigenvector matrix. Substitute equation (12) into equations (10) and (11) and multiply each of the equations by Σ^{-1}, yielding equations (13) and (14),

$$C_{liq}\frac{\partial \vec{\Phi}_{eig}}{\partial t} = C_{liq}\Lambda\frac{\partial^2 \vec{\Phi}_{eig}}{\partial r^2} \ . \tag{13}$$

Where $\vec{\Phi}_{eig} = \Sigma^{-1}\vec{\Phi}$ and $\vec{\Omega}_{\Phi,eig} = \Sigma^{-1}\vec{\Omega}_{\Phi}$. The boundary can be transformed in a similar manner yielding:

$$\left.\frac{\partial \vec{\Phi}_{eig}}{\partial r}\right|_{r=0} = 0 \ , \ C_{liq}\Lambda\left.\frac{\partial \vec{\Phi}_{eig}}{\partial r}\right|_{r=R} = \vec{\Omega}_{\Phi,eig} \ . \tag{14}$$

Since Λ is diagonal, equation (13) is a system of uncoupled partial differential equations. Each of the component equations takes the form of pseudo-diffusion of a binary mixture and thus could be solved as a pseudo-binary type problem. For component *j*, the transformed equation is given by,

$$C_{liq}\frac{\partial \Phi_{eig,j}}{\partial t} = C_{liq}\Lambda_j\frac{\partial^2 \Phi_{eig,j}}{\partial r^2} \ , \tag{15}$$

and the boundary conditions are given by,

$$\left.\frac{\partial \Phi_{eig,j}}{\partial r}\right|_{r=0} = 0 \ , \ C_{liq}\Lambda_j\left.\frac{\partial \Phi_{eig,j}}{\partial t}\right|_{r=R} = \Omega_{\Phi,eig,j} \ , \tag{16}$$

where λ_j is the j^{th} eigenvalue of the diffusivity matrix.

These equations are in the same form as those for a discrete multi-component fuel representation by Zeng and Lee [27] if the first and second moments of the probability distribution function are considered as two "discrete components". It is possible to find a relation between the surface and average properties of a droplet to approximate the effect of finite diffusion rate in the liquid phase by using the same approach as Zeng and Lee [27]: first, apply the quasi-steady state assumption and obtain an analytical solution of Equation (5). Then, obtain the transient part of the solution by separation of variables and retain only the first order term in the series solution. Finally, an approximate solution is derived using the initial condition. With this approximate solution, an expression for the difference between the surface and mean values can be obtained. The time differential form of this expression is

$$\frac{d\vec{\Phi}_{\Delta}}{dt} = \frac{\lambda_1^2}{R^2}D_{eff}\left(\frac{R}{5}D_{eff}^{-1}\vec{\Omega}_{\Phi} - \left[\mathrm{I} + \frac{Pe_v}{\lambda_1^2}\right]\vec{\Phi}_{\Delta}\right) , \tag{17}$$

where $\Phi_{\Delta} = \Phi_{r=R} - \Phi_{mean}$ (the difference between the surface and mean values), $\lambda_1 = 4.4934$, $D_{eff} = \Xi^{-1}(Pe_v)\,D$, $\dot{R}$ is the regression rate of the droplet and $\Xi^{-1}(Pe_v)$ is the enhancement coefficient for droplet surface regression, which is defined by Zeng and Lee [6] as:

$$\Xi(Pe_v) = [\varepsilon^{-1}(1, Pe_v)][\ \varepsilon(r, Pe_v)] \ , \tag{18}$$

$$\varepsilon(r,Pe_v) = \left[r^{-2}\exp\left(\frac{r^2}{2}Pe_v\right)\right]\left[\int_0^r \chi^2\exp\left(-\frac{\chi^2}{2}Pe_v\right)d\chi\right] , \tag{19}$$

$$Pe_v = -R\,\frac{dR}{dt}\,D^{-1} \ . \tag{20}$$

The average values of the moments and temperature in the liquid phase are determined by:

$$\frac{d}{dt}\left(C_{liq}R^3\,\Phi_{mean}\right) = -3R^2\,\dot{N}_{\Phi}'' \ , \tag{21}$$

$$\frac{d}{dt}\left(C_{liq}R^3\,C_{p,liq}\,T_{liq,mean}\right) = 3R^2\,\dot{q}'' \ . \tag{22}$$

Where the fluxes are given by the gas phase sub-model. Thus, the surface value can be obtained.

Results and Discussion

Model Verification

The evaporation of a pure n-decane ($C_{10}H_{22}$) droplet under the condition prescribed in Wong and Lin [28] was simulated with the proposed model. In the study by Wong and Lin [28], the droplets were suspended from a ceramic suspender. Droplet temperatures were measured by chromle-alumel thermocouples. The uncertainty in temperature measurements was ±1 K. A video recorder was used in the experiment to record the change of droplet radius. The initial diameter and temperature of the droplet were 1961 μm and 313 K, respectively. The droplet was evaporating in air moving at 1 m/s. Ambient condition was 101 kPa and 1000 K, respectively. Pure n-decane was represented by a narrow distribution with mean of 142.3 g/mol and standard deviation of 1 g/mol, and the origin (γ) of the distribution function was 132.3 g/mol. Figure 1 compares the normalized droplet radius. The proposed model predicted the variation of droplet radius well, albeit with slight discrepancy from 2 seconds onward.

Similar calculations were carried out for heptane-decane droplets evaporating in moving air. Heptane-decane droplets evaporating in ambient air of 101 kPa and 348 K were simulated. The free stream velocity of the ambient air was 3.1 m/s. Droplets of two different compositions, one composed of 75% heptane and 25% decane with initial diameter of 1484 μm and another one composed 25% heptane and 75% decane with initial diameter of

1360 µm, were simulated and compared with experimental data adopted from Daïf et al. [29]. Figure 2 shows the variation of normalized surface area both droplets. The proposed results predicted the surface regression process well. For the 75% decane droplet, the rate of surface regression was almost constant and resembled that of pure decane [29]. Note that the liquid phase was dominated by decane rapidly after evaporation started. A two-stage process was observed for the 75% heptane droplet.

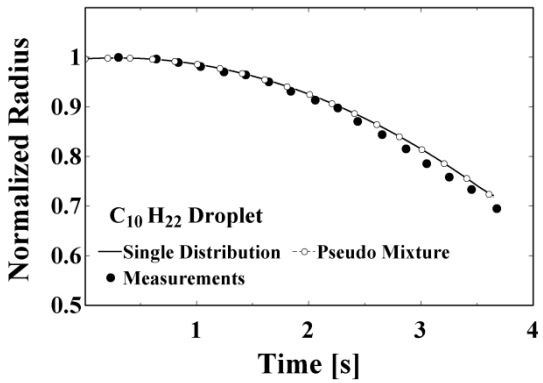

Figure 1. Normalized droplet radius for a n-decane droplet with initial radius of 980.5 µm, at 101 kPa and 1000 K. Initial droplet temperature is 313 K. Experimental data are taken from Wong and Lin [28].

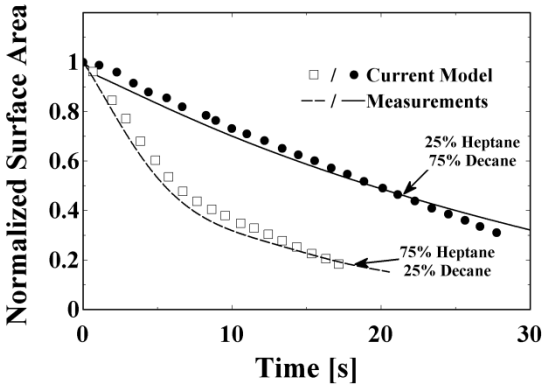

Figure 2. Variation of droplet surface area for heptane-decane droplets evaporating at ambient air of 101 kPa and 348 K. Air velocity is 3.1 m/s. Experimental data are adopted from Da f et al. [29].

Evaporation at Low Ambient Pressure

The evaporation of 50 µm gasoline-kerosene and diesel-kerosene droplets vaporizing in quiescent ambient air of 1000 K and 405 kPa were simulated. Each component constitutes 50% by mole in the mixture. The probability distributions for the three fuels are depicted in Figure 3. The distributions for kerosene and diesel overlap with each other, except the spread of the kerosene distribution was smaller. The distribution of gasoline did not overlap with the other fuels except the tail part.

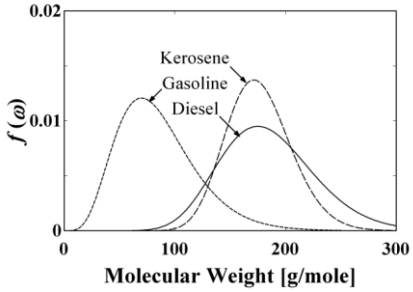

Figure 3. The probability distributions of diesel, gasoline and kerosene.

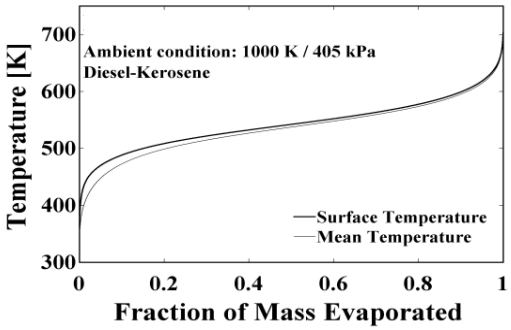

Figure 4a. Temperature variation of a 50 µm 50% diesel – 50% kerosene (by mole) droplet.

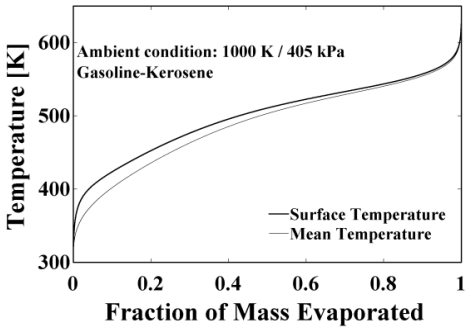

Figure 4b. Temperature variation of a 50 µm 50% gasoline – 50% kerosene (by mole) droplet.

Figure 4 shows that the mean temperature was lower than the surface temperature, especially during initial heat-up of the droplet, but the two values converged as the droplets evaporate. The predicted lifetime for the droplet was 11.4 ms. The liquid phase and vapor phase fuel composition for the gasoline-kerosene droplet are

depicted in Figure 5. From Figure 3, gasoline was more volatile than kerosene. From Figure 6, showing the liquid phase distributions of gasoline and kerosene, showed that the gasoline distribution shifting much faster than its counterparts. The liquid phase gasoline composition at droplet surface steadily decreased for the duration of droplet life. By the time when 30% of droplet mass evaporation, most of gasoline has evaporated and the droplet consisted 90% of kerosene. Gasoline was effectively depleted at about 50% of droplet mass evaporation. Note that at 75% of droplet mass evaporation, the gasoline distribution overlapped with the kerosene distribution. The mean of the gasoline distribution surpassed that of kerosene right before complete evaporation of the droplet. The fuel vapor remained almost purely kerosene due to the liquid composition at the times. This showed the interactions and effects of overlapping distribution functions on the evaporation process.

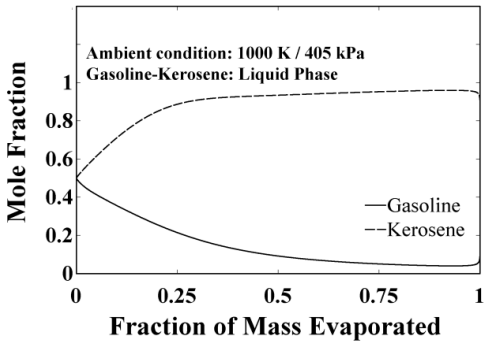

Figure 5a. Liquid phase fuel composition at droplet surface for a gasoline-kerosene droplet evaporating in quiescent ambient air at 1000 K and 405 kPa.

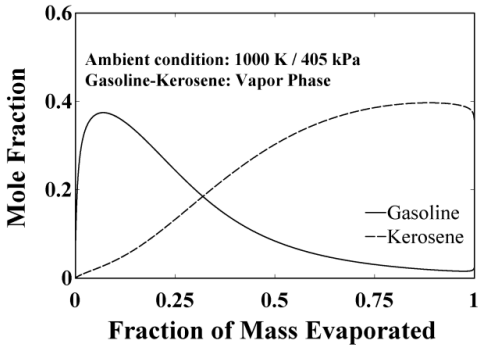

Figure 5b. Vapor phase fuel composition at droplet surface for a gasoline-kerosene droplet evaporating in quiescent ambient air at 1000 K and 405 kPa.

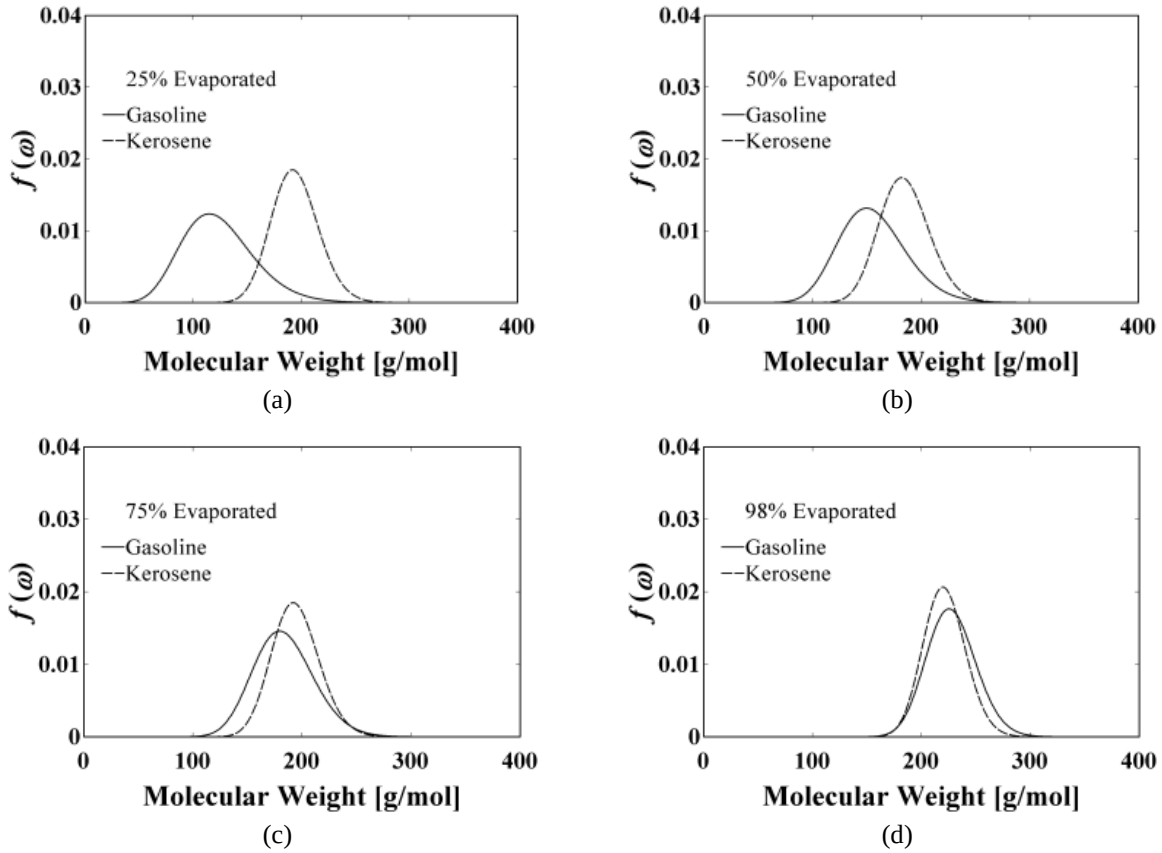

Figure 6. Liquid phase probability distributions for gasoline-kerosene droplet at (a) 25%, (b) 50%, (c) 75% and (d) 98% of droplet mass evaporation.

Summary and Conclusions

A new, comprehensive and computationally efficient model for preferential vaporization for droplets using a continuous thermodynamics formulation was developed in this study, using an approach similar to that of Wang

[20], but is more general and capable of accommodating the application of multiple probability distribution functions. The proposed model predicted the temperature and droplet size variations well by comparing with experiments. The present model was applied to simulate the evaporation of isolated droplets with composition of typical diesel. Computations showed that the model captured the main distillation characteristics of commercial fuels reasonably well. The results showed that liquid phase model would affect the predicted evaporation behavior of the droplets. Using a continuous representation of diesel, the droplet never reached an equilibrium temperature during its lifetime. The vapor phase mean composition increased and converged towards the initial liquid value as the droplet evaporated. The droplet lifetime using the continuous representation was, in general, longer than that using a single-component representation. This was true in particular for a droplet composed of non-volatile compounds. The representation of fuel could have a significant effect on the fuel vapor composition on the droplet surface. The present vaporization model was zero-dimensional with a very low computational cost, while maintaining a satisfying level of accuracy and the underlying physics of the evaporation process.

The model was applied to study the evaporation of gasoline-kerosene and diesel-kerosene mixture droplets. The distributions of gasoline and kerosene only overlapped in the tail regions. Initially, gasoline contained the most volatile components in the mixture. The mean and standard deviation of the distribution with broader spread shifted much faster than the one with narrow spread, in this case, gasoline and diesel. Upon complete droplet evaporation, the kerosene became the most volatile component in the mixture. The shifting of the distribution functions affected the rate of evaporation and also the vapor composition. The gasoline-kerosene droplet evaporated in a two-stage manner, with gasoline evaporated first, followed by kerosene. Although kerosene became the most volatile (lightest) components in the mixture by the end of the droplet life, the fuel vapor consisted mainly of gasoline or diesel because of the liquid composition at that instant.

Acknowledgements

This work was supported in part by the Department of Energy Grant No. DE-FC26-05NT42634, and by Department of Energy GATE Centers of Excellence Grant No. DE-FG26-05NT42622.

References

[1] C. K. Law, Prog. Energ. Combust., 8 (1982) 171.
[2] W. L. H. Hallett and M. A. Ricard, Fuel, 71 (1992) 225-229.
[3] E. C. Robert, E. D. John, M. G. Robert and T. D. Dan, SAE paper 980510 (1998).
[4] J. Tamim and W. L. H. Hallett, Chem. Engng. Sci., 50 (1995) 2933-2942.
[5] W. L. H. Hallett, Combust. Flames, 121 (2000) 334-344.
[6] S. Zhu and R. D. Reitz, J. Eng. Gas Turbines Pwer, 123 (2001) 412-418.
[7] A. M. Lippert and R. D. Reitz, SAE Paper 972882 (1997).
[8] G. S. Zhu and R. D. Reitz, Int. J. Heat Mass Transf., 45 (2002) 495-507.
[9] L. Zhang and S. C. Kong, Chem. Eng. Sci., 64 (2009) 3688-3696.
[10] Y. Ra and R. D. Reitz, Int. J. Engine Res., 4 (2003) 193-218.
[11] C. F. Lee, W. L. Cheng and D. Wang, Proc. Combust. Inst., 32 (2009) 2801-2808.
[12] C. Fieberg, L. Reichelt, D. Martin, U. Renz, and R. Kneer, International Journal of Heat and Mass Transfer, 52 (2009), 3738-3746.
[13] H. Ghassemi, S. W. Baek, and Q. Khan, Combustion Science and Technology, 178 (6) (2006)1031-1053.
[14] H. Ghassemi, S. W. Baek, and Q. S. Khan, Combustion Science and Technology, 178 (9) (2006), 1669-1684.
[15] S. D. Givler, and J. Abraham, Progress of Energy and Combustion Science, 22 (1996) 1-28.
[16] T. B. Gradinger, and K. Boulouchos, International Journal of Heat and Mass Transfer, 41 (1998), 2947-2959.
[17] G. S. Zhu, and S. K. Aggarwal, International Journal of Heat and Mass Transfer, 43 (7) (2000), 1157-1171.
[18] G. S. Zhu, and S. K. Aggarwal, Journal of Engineering for Gas Turbines and Power, 124 (2000), 248-255.
[19] S. Tonini, M. Gavaises, and A. Theodorakakos, International Journal of Thermal Sciences, 48 (3) (2009), 554-572.
[20] D. Wang and C. F. Lee, Proceedings of 15th ILASS Americas (2002).
[21] B. Abramzon and W. A. Sirignano, Int. J. Heat Mass Transf., 32 (1989), 1605-1618
[22] D. Jin and G. L. Borman, SAE Paper 850264 (1985).
[23] A. Y. Tong and W. A. Sirignano, Combust. Flame, 66 (1986) 221-235.
[24] H. L. Toor, AIChE Journal, 10 (1964), 448-455 and 460-465.
[25] W. E. Stewart, and R. Prober, Industrial and Engineering Chemistry Fundamentals, 3 (1964), 224-235.
[26] H. T. Cullinan, Industrial & Engineering Chemistry Fundamentals, 4 (1965), 133-139.
[27] Y. Zeng and C. F. Lee, ASME Journal of Engineering for Gas Turbines and Power, 124 (2002), 717-724.

[28] S. C. Wong, and A. C. Lin, Journal of Fluid Mechanics, 237 (1992), 671-687.
[29] A. Daïf, M. Bouaziz, X. Chesneau, and A. A. Chérif, Experimental Thermal and Fluid Science, 18 (1999), 282-290.